Interaction of W(CO)$_6$ with SiO$_2$ surfaces: A density functional study

Kaliappan Muthukumar, Ingo Opahle, Juan Shen, Harald O. Jeschke, and Roser Valentí

Institut für Theoretische Physik, Goethe-Universität Frankfurt, Max-von-Laue-Straße 1, D-60438 Frankfurt am Main, Germany

The interaction of tungsten hexacarbonyl [W(CO)$_6$] precursor molecules with SiO$_2$ substrates is investigated by means of density functional theory calculations with and without inclusion of long-range van der Waals interactions. We consider two different surface models, a fully hydroxylated and a partially hydroxylated SiO$_2$ surface, corresponding to substrates under different experimental conditions. For the fully hydroxylated surface, we observe only a weak interaction between the precursor molecule and the substrate, with physisorption of W(CO)$_6$. Inclusion of van der Waals corrections results in a stabilization of the molecules on this surface, but does not lead to significant changes in the chemical bonding. In contrast, we find a spontaneous dissociation of the precursor molecule on the partially hydroxylated SiO$_2$ surface, where chemisorption of a W(CO)$_5$ fragment is observed upon removal of one of the CO ligands from the precursor molecule. Irrespective of the hydroxylation, the precursor molecule prefers binding of more than one of its CO ligands. In light of these results, implications for the initial growth stage of tungsten nanodeposits on SiO$_2$ in an electron-beam-induced deposition process are discussed.

PACS number(s): 68.43.Fg, 71.15.Mb, 71.15.Nc

I. INTRODUCTION

The growth of patterned transition metal nanodeposits with tunable electronic properties has been in the focus of recent research toward nanoscale device applications.[1,2] One of the promising routes to achieve this goal is the preparation of nanodeposits from gas phase precursor molecules like tungsten hexacarbonyl [W(CO)$_6$] or cyclopentadienyltrimethylplatinum(IV) by means of focused ion- or electron-beam-induced deposition (EBID) or laser-induced deposition techniques.[2–4] While experimentally substantial progress has been made in the fabrication of transition metal nanodeposits with properties reaching from insulating to metallic or even superconducting behavior,[5] a detailed understanding of the growth processes on a microscopic level is still missing. This is due to the multitude of complicated processes involved in the growth of nanodeposits from the gas phase—like the adsorption or chemisorption of precursor molecules, heat transfer, and the interaction with primary and secondary electrons in the EBID process, as well as fragmentation and recombination of fragments—which do not allow a one-step simulation of the growth process within reasonable time.

W(CO)$_6$ is one of the most prominent precursor materials used in the EBID process and has been deposited on various substrates like SiO$_2$,[6,7] W(110),[8] and Ni(100),[9] by use of a variety of techniques. The chemical and physical properties of W(CO)$_6$ as a molecule are well studied both experimentally and theoretically.[9–15] However, to the best of our knowledge, there have been no reports of electronic structure calculations that treat the interaction of W(CO)$_6$ molecules with the SiO$_2$ substrate. Therefore, in this work, we focus on constructing a reasonable model for the SiO$_2$ substrate and study the interaction of a single W(CO)$_6$ molecule with the SiO$_2$ substrate as one important step toward the simulation of a realistic growth process in EBID.

For the simulation of the W(CO)$_6$ interaction with the SiO$_2$ substrate, we employ two different surface models, a fully hydroxylated (FOH) and a partially (POH) hydroxylated SiO$_2$ surface. The FOH SiO$_2$ represents a realistic model

for a substrate prepared under nonvacuum conditions in the absence of irradiation, while the POH SiO$_2$ corresponds to a substrate under the influence of an electron beam, where a partial removal of OH groups from the surface is expected due to the interaction with the beam, as on other surfaces such as TiO$_2$ and γ-Al$_2$O$_3$.[16,17] The interaction between the precursor molecule and the substrate is then studied within density functional theory (DFT) using the generalized gradient approximation (GGA) with and without van der Waals (vdW) interactions. The impact of vdW interactions, which were found to be important for the interaction of organic molecules on metal surfaces in recent studies,[18,19] is discussed for the present system.

II. COMPUTATIONAL DETAILS

DFT calculations for bulk SiO$_2$, isolated SiO$_2$ substrates, and W(CO)$_6$ precursor molecules, as well as the combined substrate–precursor molecule system were performed using the projector augmented wave method[20,21] as implemented in the Vienna *ab initio* simulation package (VASP version 5.2.11).[22–24] The GGA in the parametrization of Perdew, Burke, and Ernzerhof[25,26] was used as approximation for the exchange and correlation functional. In addition, dispersion corrections[27,28] were used that simulate the long-range vdW interactions, which are expected to be important for the adsorption of the W(CO)$_6$ molecules on the FOH SiO$_2$ surface.

For bulk SiO$_2$, the ideal β-cristobalite structure[29] with cubic $Fd\bar{3}m$ symmetry [Fig. 1(a)] and the experimental lattice constant $a = 7.16$ Å was used. To simulate the substrate-precursor interaction, slabs consisting of two to five layers of SiO$_2$ with a hexagonal SiO$_2$(111) surface were generated from the experimental bulk structure. The minimal slab geometry to simulate the hexagonal SiO$_2$(111) surface has in-plane lattice parameters corresponding to the primitive lattice constants $a_p = a/\sqrt{2} = 5.06$ Å of the face-centered cubic cell. This minimal geometry, however, does not allow for a sufficient separation of adjacent images when the molecule is placed
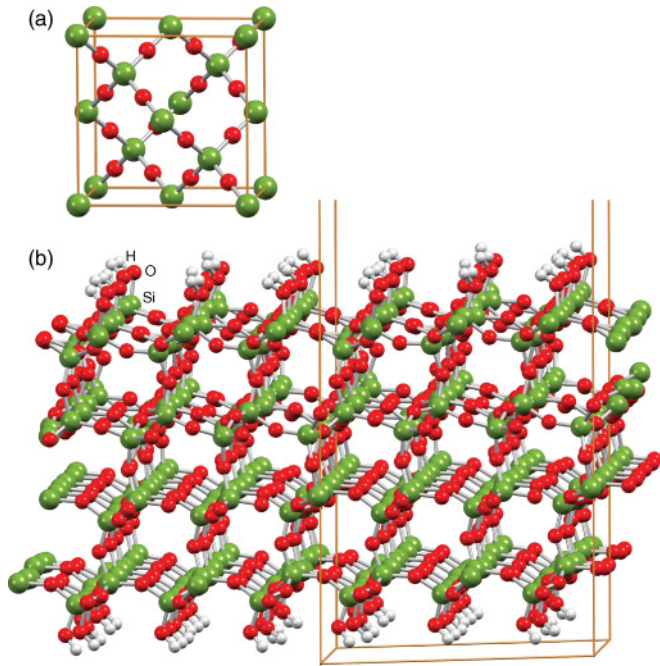
FIG. 1. (Color online) (a) Structure of bulk β-cristobalite SiO_2 and (b) side view of the slab geometry with a (111) surface used for this study. The corresponding unit cell is indicated.

on the surface. Thus we used a 3×3 supercell geometry in the plane (in terms of primitive lattice constants) for all slab calculations.

For the FOH SiO_2 substrate, all surface silicon atoms (top and bottom) were terminated with OH groups [Fig. 1(b)]. In the case of the POH SiO_2 surface, some of the OH groups were removed from this slab. We considered three cases depending on the precursor molecule orientation with OH-vacancy concentrations of 11%, 22%, and 33%. Both the FOH SiO_2 and POH SiO_2 substrates were then optimized. In the next step, we considered the $W(CO)_6$ molecule in similar orientations for both classes of substrates; the corresponding geometries were then reoptimized with fixed in-plane lattice parameters but otherwise no symmetry constraints, and the energies were compared after relaxation. All calculations which involve the bonding of the precursor molecules to the substrate were carried out in a four-layered 3×3 supercell geometry in the plane perpendicular to the surface, corresponding to a low coverage of precursor molecules in the initial growth stage. The choice of the 3×3 supercell geometry (with up to 256 atoms for the substrate-precursor system) allows for a distance of more than 8 Å between two precursor molecules (when measured between the two CO ligands of the adjacent molecules), thus providing an optimal compromise between computational effort and minimization of the interaction between the precursor molecules. In all cases, the distance between slabs (on the c axis) was kept large enough (30 Å, which provides a distance of 24 Å on the substrate-precursor system) to prevent significant interactions between the adjacent images.

All calculations were performed in the scalar relativistic approximation. A kinetic energy cutoff of 400 eV was used, and all ions were fully relaxed using a conjugate gradient

scheme until the forces were less than 0.01 eV/Å. In the geometry optimizations for the molecule and the surface models, the Brillouin zone was sampled at the Γ point only. For the final comparison of energies and the density of states (DOS), a **k** mesh of $4 \times 4 \times 1$ has been used for the slabs, showing a convergence of the total energy to about 10^{-4} eV/f.u. For bulk SiO_2 the **k**-point sampling was performed with a $16 \times 16 \times 16$ Monkhorst-Pack grid. For all DOS calculations, a Gaussian broadening of 20 meV was applied. Spin polarization was considered for all calculations. Different spin states for each cluster-adsorbate system were checked (i.e., in each case the two lowest possible spin states) and only the results of the ground state are reported below.

In addition, the $W(CO)_6$ molecule was optimized in the O_h symmetry in a cubic box of 30 Å, and the structural parameters were used to compare with the surface models. We also analyzed the electronic orbitals with TURBOMOLE 6.0,[30,31] using the triple-zeta valence plus polarization (def-TZVP) basis sets, the same GGA functional as for the bulk calculations, and the resolution of identity approximation. In this case, an effective core potential has been used for W, which provides 12 active valence electrons.

The adsorption energy was defined as $\Delta E = E_{total} - E_{substrate} - E_{adsorbate}$, where E_{total}, $E_{substrate}$, and $E_{adsorbate}$ are the energies of the combined system (adsorbate and cluster), of the cluster, and of the adsorbate molecule in the gas phase in a neutral state, respectively.

III. RESULTS

A. Electronic structure of the SiO_2 substrate

SiO_2 exists in a variety of crystalline and amorphous modifications. In most experimental studies, amorphous SiO_2 substrates are used for the growth process, which are however very demanding for the computational simulations. Therefore we use in our study β-cristobalite, which resembles most closely amorphous SiO_2, as a representative structure for amorphous SiO_2. Experimental studies have shown that β-cristobalite and amorphous SiO_2 have a very similar local structure and exhibit similar physical properties such as density and refractive index.[32] Following Refs. [33]–[36], we use the ideal β-cristobalite structure with $Fd\bar{3}m$ symmetry.

It has been reported that the silica surface may contain segments of surfaces resembling both the (111) and (100) faces of cristobalite.[37,38] The Bravais-Donnay-Friedel-Harker method provides an estimate of the relative growth rates of the possible faces of each crystal structure and the resultant morphology, which shows that there exists only one dominant plane for SiO_2, which is (111).[39] Therefore, the surface of the substrate is simulated by the (111) plane of bulk β-cristobalite.

For a slab size of four layers we have observed a convergence in structural and electronic properties. In the optimized structure of four-layer slabs with no symmetry constraints, the bond lengths of Si and O in the inner two layers are found to be in the range of 1.62–1.63 Å, matching well with the experimental values of 1.61 Å,[40] and previously reported theoretical values.[41] Figure 2 shows the DOS of bulk SiO_2 (upper panel) and the DOS of the FOH SiO_2 four-layer slab
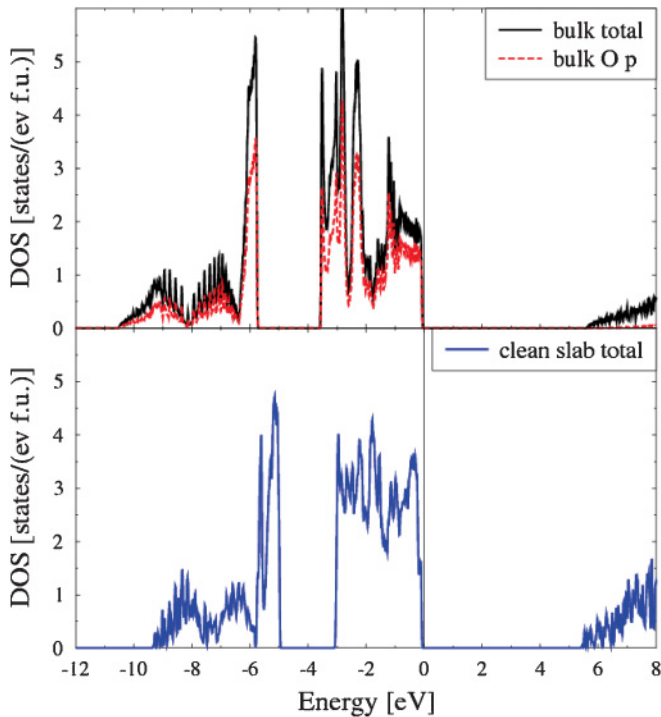
FIG. 2. (Color online) DOSs of bulk SiO$_2$ (top) in comparison to the OH-terminated four-layer slab (bottom). Shown are the total DOS (solid line) and the partial O $2p$ contribution for the bulk (dashed line). Results are shown for GGA calculations without vdW corrections.

(lower panel). The upper valence bands in the region between -10 and 0 eV below the Fermi energy are dominated by O $2p$ states with some admixture of Si states (not shown). The electronic structure of the four-layer slab shows a reasonable convergence with respect to the bulk (note that there are some smaller differences due to finite-size and relaxation effects as well as due to different **k**-point sampling, which, however, should not affect the discussions in the subsequent sections).

B. Electronic structure of W(CO)$_6$ in the gas phase

The structural and electronic properties of W(CO)$_6$ have been widely investigated using local basis sets over the last two decades.[42,43] To compare the electronic and energetic properties of W(CO)$_6$ both in the gas phase and as an adsorbed species, we have optimized the structure using a plane-wave basis set. The optimized structure is shown in Fig. 3(a). The calculated W-C bond length of the free molecule obtained using a plane-wave basis is found to be 2.06 Å and the C-O bond length is 1.16 Å, compared to 2.06 Å and 1.15 Å, respectively, determined in experiment.[44,45] Investigation of the electronic structure of W(CO)$_6$ shows that the highest occupied state is dominated by W $5d$ orbitals. Indeed, the analysis of molecular orbitals also confirms this fact. The highest occupied molecular orbital (HOMO) and the lowest unoccupied molecular orbital (LUMO) of W(CO)$_6$ are shown in Figs. 3(b) and 3(c), which show that the HOMO is made up of W $5d$ while the LUMO is dominated by p orbitals of the CO ligands.
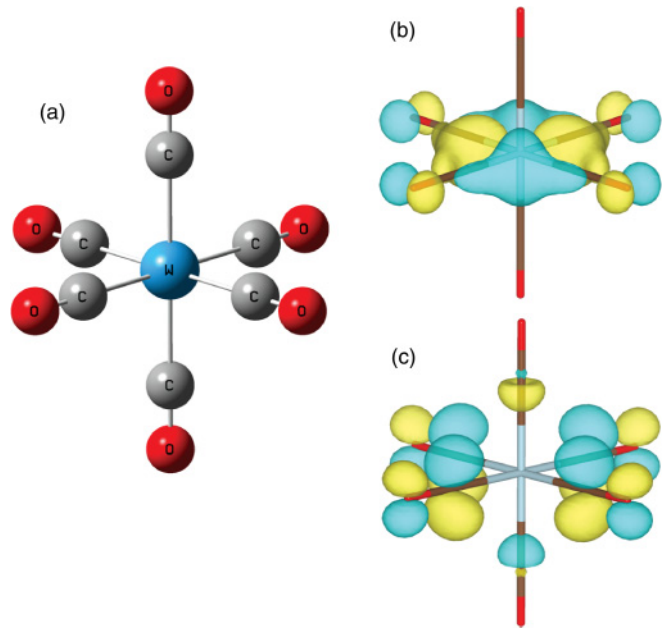

FIG. 3. (Color online) (a) Optimized structure of W(CO)$_6$ and one of its triply degenerate (b) HOMOs and (c) LUMOs shown as representatives.

C. Interaction of W(CO)$_6$ with the fully hydroxylated SiO$_2$ substrate

The FOH SiO$_2$ surface corresponds to a substrate prepared under wet-chemical conditions in the absence of an electron or ion beam. In accordance with the available experimental results, CO ligands of W(CO)$_6$ have been used to bond to the substrate.[46] Three different orientations are considered which differ in the number of CO ligands bonding to the surface. These configurations were subsequently relaxed without any symmetry constraints. A schematic representation of the three configurations considered (C1, C2, and C3; Cn involves bonding to n CO ligands) and their corresponding adsorption energies ΔE are shown in Fig. 4 (upper and lower panels).

Our results illustrate that the W(CO)$_6$ molecule bonded with two of its CO ligands to the substrate (C2) is the most stable configuration, with an adsorption energy of -0.162 eV upon neglect of vdW interactions. However, the energy difference compared to the next most stable configuration, which involves three CO ligands bonding to the substrate (C3), is quite small (about 25 meV), which may be indicative for a certain capacity of the molecule to roll over the surface. In the relaxed structure, the minimal distances observed between the molecule CO groups and the surface OH groups are 2.07 Å (C1), 2.14 Å (C2), and 2.06 Å (C3).

The weak interaction between W(CO)$_6$ and the FOH SiO$_2$ surface results only in minor rearrangements of the substrate surface geometry. For instance, the Si-O bond distance on the adsorbate-free surface is in the range of 1.62–1.65 Å. For the relaxed configuration with adsorbate, we do not observe any significant changes of these distances, illustrating the fact that the surface does not contribute significantly to the bonding. We also observe only minor changes in the structure of the W(CO)$_6$ molecule bonded to the surface. In all the configurations we have considered, the W-C and the C-O bonds that are involved
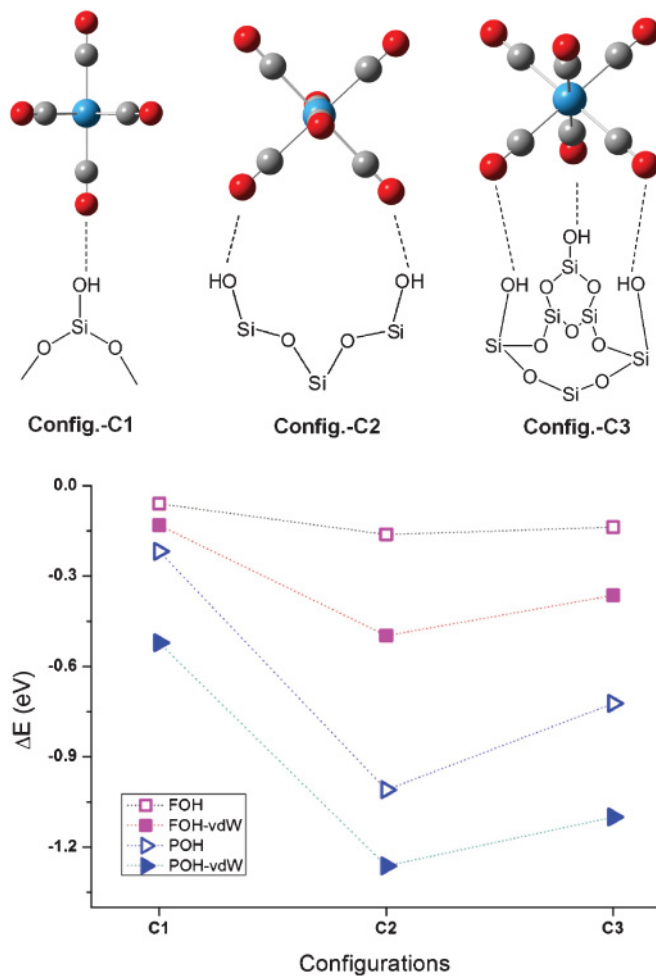
FIG. 4. (Color online) Top panel: Three different configurations of $W(CO)_6$ (C1, C2, and C3) considered for the adsorption on the FOH SiO_2 surface are shown schematically. Similar configurations are considered on the POH SiO_2 surfaces where the CO ligands bond directly to the surface Si atoms. Bottom panel: Variation of the adsorption energy ΔE for the different configurations with respect to the orientation of $W(CO)_6$. Results are shown for the FOH SiO_2 and POH SiO_2 with and without inclusion of vdW corrections.

in the bonding with the surface are shortened by 0.01–0.02 Å, which also confirms the weak adsorption.

The role of vdW forces on these adsorption geometries is evaluated by adding vdW corrections to the calculations, which are not accounted for by DFT within the GGA functional. As expected, the absolute values of the adsorption energies are increased for all probed configurations [Fig. 4 (lower panel)]. For the most stable configuration (C2), we find an adsorption energy $\Delta E = -0.498$ eV.

We observe minor changes in the structural parameters when vdW corrections are included in the calculations compared to the set of calculations without these corrections. For example, the minimal distances between the surface and the molecule in the three configurations are 2.11 Å (C1), 2.20 Å (C2), and 2.08 Å (C3), and the changes in the W-C and C-O bond lengths are very small (of the order of 0.01 Å) compared to the results of calculations without dispersion corrections.

Although the minimal distances between the molecule and the surface are similar in both cases (C2 and C3), for the preferred configuration (C2), the remaining CO ligands are found to lie closer to the surface with next-nearest distances of 2.29 and 2.65 Å [see Fig. 5(b)], compared to 2.82 and 3.43 Å [see Fig. 5(a)] when the corrections are not implemented. This in fact has an impact on the orientation of the molecule on the surface. Furthermore, the differences between the adsorption energies of the different configurations are now larger, thus indicating that vdW interactions tend to decrease the ability of the precursor molecule to spontaneously roll over the surface.

The DOS of $W(CO)_6$ on the FOH SiO_2 surface for C2 is shown in Fig. 6 (middle panel) in comparison to the DOS of the slab without adsorbate (top panel). Results are shown for calculations including vdW corrections, which, however, have only minor influence on the electronic structure [compare Fig. 2 (bottom panel)]. The highest molecular level of the $W(CO)_6$ adsorbate lies in the gap of the substrate, which pins the Fermi level close to the valence band. Thus the DOS of the SiO_2 substrate consisting mostly of O p states is shifted to lower energies with respect to the Fermi energy. Otherwise, the DOS of the SiO_2 substrate shows only minor modifications with respect to that of the free substrate. The molecular levels of the $W(CO)_6$ adsorbate are visible in sharp peaks and agree well with the energetic levels of the free $W(CO)_6$ molecule obtained by our TURBOMOLE calculations (also shown in the top panel of Fig. 6). This further illustrates the weak interaction between the adsorbate molecule and the SiO_2 substrate.

D. Interaction of $W(CO)_6$ with the partially hydroxylated SiO_2 substrate

Partial dehydroxylation of the surface of a wet-chemically prepared SiO_2 substrate is expected to occur under irradiation with an electron or ion beam or at elevated temperatures. To represent this situation in this study, we kept the Si atoms bonding to CO ligands unterminated, while all other dangling bonds of Si on the two surfaces of the slab were terminated by OH groups. The $W(CO)_6$ molecule was placed in such a way that it bonds with one, two, or three CO ligands to the unterminated Si surface atom and the substrate-precursor system was subsequently relaxed.

Our results indicate that the $W(CO)_6$ molecule is adsorbed more strongly on the POH SiO_2 surface in all three orientations compared to the FOH SiO_2 surface (see Fig. 4, lower panel). Also on the POH SiO_2 surface the precursor molecule prefers to be bonded through multiple CO ligands. In the multiple-bonding configurations (C2 and C3), we observe a spontaneous fragmentation of the $W(CO)_6$ precursor molecule with chemisorption of a $W(CO)_5$ fragment on the surface upon removal of one of the CO ligands.

The most stable configuration (C2) after relaxation with $\Delta E = -1.010$ eV upon neglect of vdW interactions is shown in Fig. 5(c). The fragmented CO lies at a distance of 4.15 Å from the subcarbonyl moiety (measured between "W" and CO) and 5.03 Å from the surface (measured between C and the nearest H atom of the surface OH group) and remains as a free CO molecule. The bond distances between Si and the O atoms of the CO ligands involved in the bonding are about 1.71 Å and quite close to the Si-O bond lengths of 1.62–1.65 Å observed in
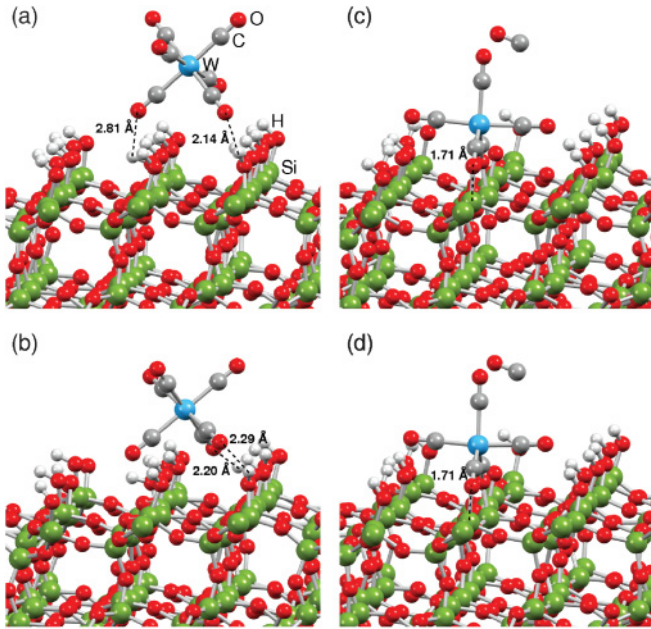
FIG. 5. (Color online) Illustration of the role of the vdW correction in determining the bonding of W(CO)$_6$ (C2) to the FOH SiO$_2$ (a),(b) and POH SiO$_2$ (c),(d) surfaces. The upper panels (a) and (c) correspond to calculations without vdW corrections while the relaxed structures in the lower panels (b) and (d) include vdW corrections.

FIG. 6. (Color online) DOS of W(CO)$_6$ on SiO$_2$ in comparison to that of the clean SiO$_2$ surface. Shown are the total DOS (solid lines) along with the partial contributions of the adsorbate (dashed lines) for the preferential configurations on the POH SiO$_2$ surface (bottom panel) and on the FOH SiO$_2$ surface (middle panel). The top panel shows the total DOS of the SiO$_2$ surface (solid line) along with the energetic levels of the free W(CO)$_6$ molecule. The Fermi energy is set to zero.

various compounds,[47] indicating a nearly optimal interaction. The distances from the O atoms of the two nonbonding CO ligands to the H atoms of the OH group are 1.94 and 1.98 Å, indicating the presence of a weak interaction which might also stabilize the molecule on the surface.

A similar effect is also seen for the singly coordinated system (C1). When the W(CO)$_6$ molecule is bonded by only one of its CO ligands to the POH SiO$_2$ surface, the distance between Si and O of the nearest CO ligand is 1.73 Å, with the fairly small adsorption energy $\Delta E = -0.218$ eV. The distances of nonbonding CO ligands from the substrate are 2.31 and 2.58 Å, compared to 2.08–2.48 Å found for FOH SiO$_2$ surfaces. In the three-coordinated system (C3), where the W(CO)$_6$ molecule is bonded by three of its CO ligands to the POH SiO$_2$ surface, the Si-O (of CO) distances range from 1.69 to 1.70 Å with an adsorption energy ΔE of -0.723 eV.

In the preferred configuration (C2), the W-C bond lengths of 1.87–1.94 Å for the CO groups which are involved in the bonding to the substrate are shorter compared to the value found in the gas phase, 2.05 Å. On the other hand, the bond lengths of the nonbonding CO ligands are slightly elongated (2.11–2.12 Å), illustrating a weakening of these bonds.

Calculations have also been carried out by including vdW corrections. No major changes are observed in the structural parameters of W(CO)$_6$ [see also Figs. 5(c) and 5(d)]. However, differences are observed for the calculated ΔE on these POH SiO$_2$ surfaces (Fig. 4, lower panel). The most stable configuration (C2) has an adsorption energy $\Delta E = -1.262$ eV when vdW interactions are included. Moreover, the differences in ΔE between bi- and tricoordinate orientation of W(CO)$_6$ on these surfaces become small, illustrating the presence of physisorption although dominated by chemisorption in these
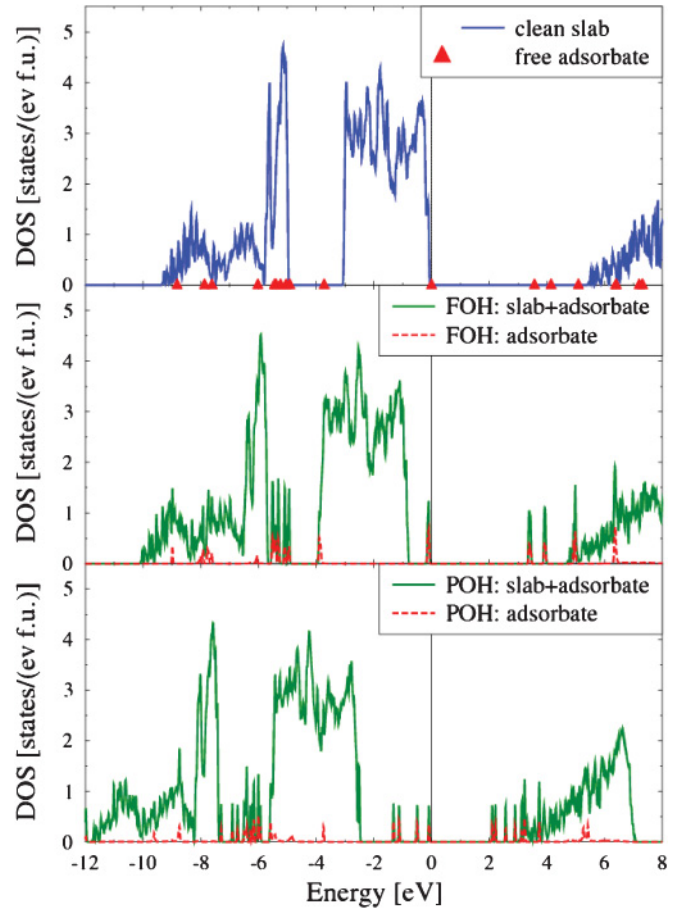
cases. Irrespective of either the orientation or the inclusion of vdW corrections, fragmentation of W(CO)$_6$ molecules is found to occur.

The DOS of the preferential configuration of W(CO)$_6$ on the POH SiO$_2$ surface (C2) is shown in the bottom panel of Fig. 6. Similar to the case of W(CO)$_6$ on the FOH SiO$_2$ surface, the overall shape of the partial DOS of the substrate is only little altered by the interaction with the precursor molecule, but shifted to lower energies with respect to the Fermi level since the highest occupied level of the adsorbate lies in the gap of the substrate. However, in contrast to the result for the FOH SiO$_2$ surface, the energetic levels of the adsorbate now have little in common with those of the free gas phase W(CO)$_6$ molecule, as a consequence of the stronger interaction and the fragmentation of the precursor molecule.

In order to analyze the nature of the bonding between precursor and SiO$_2$ substrate in the adsorption process, we show in Fig. 7 the charge density of the highest occupied valence band of W(CO)$_6$ adsorbed on FOH SiO$_2$ [see Fig. 7(a)] and POH SiO$_2$ [see Fig. 7(b)] surfaces. Our results indicate that
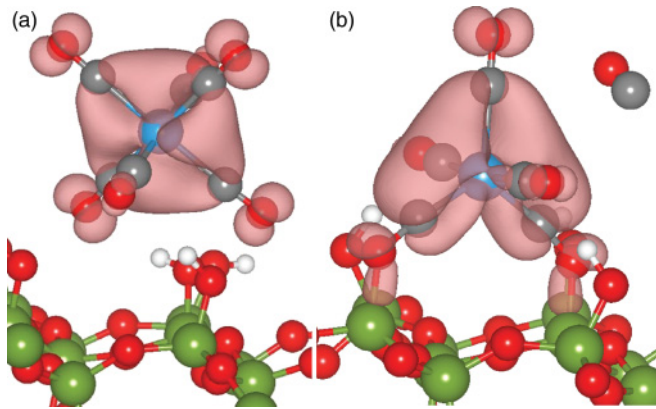
FIG. 7. (Color online) Band-decomposed charge density for the valence band maximum for the FOH SiO_2 (a) and POH SiO_2 (b) cases.

the degeneracy of the W $5d$ triply degenerate HOMO level is nearly preserved on the FOH SiO_2 surface [cf. Figs. 3(b) and 7(a)], while it is strongly altered as a consequence of the symmetry lowering while binding to the POH SiO_2 substrate [cf. Figs. 3(b) and 7(b)]. This observation illustrates the fact that the electron density on the tungsten is perturbed upon bonding to dehydroxylated Si atoms located on the SiO_2 surface, which acts as an electron accepting center.[48] Our computed Bader charges on the POH SiO_2 surface before and after bonding illustrate that the dehydroxylated Si atom on the substrate gains 0.9 electrons as a result of bonding. This interaction results in the formation of a ligand-surface adduct which destabilizes the molecule by weakening the W-CO bonds that were not involved in bonding to the substrate and ultimately eliminates one of its CO ligands. In fact, this behavior is similar to the interaction of group-VI metal carbonyls with the Al^{3+} sites of γ-Al_2O_3, resulting in the formation of subcarbonyl entities bonded to the surface.[49] Owing to the high adsorption energy, the formed subcarbonyl moiety has less mobility on the surface than the unfragmented molecule. In summary, the observation of high adsorption energy of $W(CO)_5$, the elongation of the W-CO bonds oriented toward the vacuum, and the fragmentation of one of the CO ligands on the POH SiO_2 surface confirm that $W(CO)_6$ bonds in a similar fashion on the POH SiO_2 surface as on γ-Al_2O_3.

IV. DISCUSSION: TOWARD A REALISTIC SIMULATION OF THE GROWTH PROCESS

The results obtained in the previous section show that $W(CO)_6$ is only weakly adsorbed on a FOH SiO_2 surface. The calculated adsorption energies in the range between $\Delta E \approx -0.1$ and -0.5 eV may eventually allow the growth of $W(CO)_6$ layers at low temperatures, but do not lead to the growth of metallic W deposits. Furthermore, the small energy differences between the probed configurations of $W(CO)_6$ on the FOH SiO_2 substrate are indicative of a high mobility on the surface, although the energy barriers between the configurations are hard to estimate. Experimentally, the formation of $W(CO)_6$ layers has been observed by exposure of a $TiO_2(110)$ surface to $W(CO)_6$ molecules at $T = 140$ K, which, however,

desorb again after annealing to room temperature.[50] In contrast, we observe chemisorption of $W(CO)_6$ with a spontaneous fragmentation of the precursor molecule into $W(CO)_5$ upon removal of a volatile CO ligand on a POH SiO_2 surface. The possibility of mobility on the FOH SiO_2 surfaces and fragmentation of the CO ligands on the POH SiO_2 surfaces observed in this study illustrates that the molecule may roll over to the POH SiO_2 surface regions and get activated for fragmentation.

The rate-limiting step in the decomposition of $W(CO)_6$ is believed to be the elimination of the first W-CO bond. In the gas phase, this elimination requires about 45 kcal/mol,[51,52] but is expected to be essentially smaller on the substrate and has been estimated to be about 12 kcal/mol for $W(CO)_6$ on Ni(100).[9] Further, experiments have found that complete decarbonylation occurs at around 150–205 °C in chemical vapor deposition experiments.[9,53] This, in fact, is supported by the weakening of bonds of the CO ligands not involved in the bonding to the substrate observed in our calculations, which simplifies the elimination of further ligands by thermal or radiative processes. Our results thus show that the spontaneous fragmentation of $W(CO)_6$ on a POH SiO_2 surface is a relevant process to be taken into account for the simulation of the initial stage of the growth of tungsten nanodeposits.

V. CONCLUSIONS

The interaction between a $W(CO)_6$ precursor molecule and SiO_2 substrates has been studied in the framework of density functional theory. Our results show that the interaction between the precursor molecule and the FOH SiO_2 substrate results in a weak adsorption of the precursor molecule. However, upon partial dehydroxylation of the surface, we observe a chemisorption and fragmentation of the precursor molecule, which is explained in terms of the changes of the electronic properties and the charge transfer between the precursor molecule and the substrate. We observe that vdW corrections result in a reorientation and stabilization of the molecules on the FOH SiO_2 surface but have only a minor impact on the adsorption geometry for the POH SiO_2 surface.

Our reported calculations provide insight into various aspects of the interaction of the precursor molecule with the SiO_2 substrate. In a real growth of nanodeposits, as in the case of electron-beam-induced deposition of precursor molecules on a substrate, there are a multitude of processes to be taken into account. The interaction of the beam with the precursor molecules in the gas phase, for instance, will lead to an activation or fragmentation of the precursor molecules. However, since in focused EBID experiments the fraction of gas phase molecules interacting directly with the beam is small, this process may be expected to be of minor relevance for EBID.[54] Furthermore, the interaction of the beam with the substrate will lead to heating and charging of the substrate as well as to emission of secondary electrons and photons. These processes can be partially taken into account by finite-temperature molecular dynamics simulations, which we plan to do in the future but are beyond the scope of the present investigations.

ACKNOWLEDGMENTS

[1] J. D. Wnuk, S. G. Rosenberg, J. M. Gorham, W. F. van Dorp, C. W. Hagen, and D. H. Fairbrother, Surf. Sci. **605**, 257 (2011).

[2] I. Utke, P. Hoffmann, and J. Melngailis, J. Vac. Sci. Technol. B **26**, 1197 (2008).

[3] C. R. Arumainayagam, H.-L. Lee, R. B. Nelson, D. R. Haines, and R. P. Gunawardane, Surf. Sci. Rep. **65**, 1 (2010).

[4] P. Seuret, F. Cicoira, T. Ohta, P. Doppelt, P. Hoffmann, J. Weber, and T. A. Wesolowski, PhysChemChemPhys. **5**, 268 (2003).

[5] I. Guillamón, H. Suderow, S. Vieira, A. Fernández-Pacheco, J. Sesé, R. Córdoba, J. M. De Teresa, and M. R. Ibarra, New J. Phys. **10**, 093005 (2008).

[6] H. W. P. Koops, R. Weiel, D. P. Kern, and T. H. Baum, J. Vac. Sci. Technol. B **6**, 477 (1988).

[7] F. Okuyama, Appl. Phys. Lett. **36**, 46 (1980).

[8] F. A. Flitsch, J. R. Swanson, and C. M. Friend, Surf. Sci. **245**, 85 (1991).

[9] F. Zaera, J. Phys. Chem. **96**, 4609 (1992).

[10] A. Brenner, D. A. Hucul, and S. J. Hardwick, Inorg. Chem. **18**, 1478 (1979).

[11] H. B. Linden, H. D. Beckey, and F. Okuyama, Appl. Phys. **22**, 83 (1980).

[12] A. Kuzusaka and R. F. Howe, J. Mol. Catal. **9**, 199 (1980).

[13] A. W. Ehlers and G. Frenking, J. Am. Chem. Soc. **116**, 1514 (1994).

[14] M. Kurhinen, T. Venalainen, and T. A. Pakkanen, J. Phys. Chem. **98**, 10237 (1994).

[15] M. Suvanto and T. A. Pakkanen, J. Mol. Catal. A: Chem. **138**, 211 (1999).

[16] Z. Zhang, Y. Du, N. G. Petrik, G. A. Kimmel, I. Lyubinetsky, and Z. Dohnalek, J. Phys. Chem. C **113**, 1908 (2009).

[17] Y. Wang, F. Gao, M. Kaltchev, and W. T. Tysoe, J. Mol. Catal. A: Chem. **209**, 135 (2004).

[18] N. Atodiresei, V. Caciuc, P. Lazić, and S. Blügel, Phys. Rev. Lett. **102**, 136809 (2009).

[19] N. Atodiresei, J. Brede, P. Lazić, V. Caciuc, G. Hoffmann, R. Wiesendanger, and S. Blügel, Phys. Rev. Lett. **105**, 066601 (2010).

[20] P. E. Blöchl, Phys. Rev. B **50**, 17953 (1994).

[21] G. Kresse and D. Joubert, Phys. Rev. B **59**, 1758 (1999).

[22] G. Kresse and J. Furthmüller, Comput. Mater. Sci. **6**, 15 (1996).

[23] G. Kresse and J. Hafner, Phys. Rev. B **47**, 558 (1993).

[24] G. Kresse and J. Hafner, Phys. Rev. B **49**, 14251 (1994).

[25] J. P. Perdew, K. Burke, and M. Ernzerhof, Phys. Rev. Lett. **77**, 3865 (1996).

[26] J. P. Perdew, K. Burke, and M. Ernzerhof, Phys. Rev. Lett. **78**, 1396 (1997).

[27] S. Grimme, J. Comput. Chem. **27**, 1787 (2006).

[28] X. Wu, M. C. Vargas, S. Nayak, V. Lotrich, and G. Scoles, J. Chem. Phys. **115**, 8748 (2001).

[29] R. W. G. Wyckoff, *Crystal Structures* (John Wiley & Sons, New York, 1963), Vol. 1, pp. 318–319.

[30] O. Treutler and R. Ahlrichs, J. Chem. Phys. **102**, 346 (1995).

[31] K. Eichkorn, F. Weigend, O. Treutler, and R. Ahlrichs, Theor. Chem. Acc. **97**, 119 (1997).

[32] D. E. Jiang and E. A. Carter, Phys. Rev. B **72**, 165410 (2005).

[33] T. O. Wehling, A. I. Lichtenstein, and M. I. Katsnelson, Appl. Phys. Lett. **93**, 202110 (2008).

[34] F. Vigné-Maeder and P. Sautet, J. Phys. Chem. B **101**, 8197 (1997).

[35] D. Ceresoli, M. Bernasconi, S. Iarlori, M. Parrinello, and E. Tosatti, Phys. Rev. Lett. **84**, 3887 (2000).

[36] D. Ricci and G. Pacchioni, Phys. Rev. B **69**, 161307(R) (2004).

[37] J. B. Peri and A. L. Hensley Jr., J. Phys. Chem. **72**, 2926 (1968).

[38] D. W. Sindorf and G. E. Maciel, J. Am. Chem. Soc. **105**, 1487 (1983).

[39] E. Puhakka, M. Riihimäki, M. T. Pääkkönen, and R. L. Keiski, Heat Transfer Eng. **32**, 282 (2011).

[40] A. F. Wright and A. J. Leadbetter, Philos. Mag. **31**, 1391 (1975).

[41] J. Yang, S. Meng, L. Xu, and E. G. Wang, Phys. Rev. B **71**, 035413 (2005).

[42] A. Rosa, E. J. Baerends, S. J. A. van Gisbergen, E. van Lenthe, J. A. Groeneveld, and J. G. Snijders, J. Am. Chem. Soc. **121**, 10356 (1999).

[43] K. Liu, C. G. Ning, Z. H. Luo, L. L. Shi, and J. K. Deng, Chem. Phys. Lett. **497**, 229 (2010).

[44] L. O. Brockway, R. V. G. Ewens, and M. W. Lister, Trans. Faraday Soc. **34**, 1350 (1938).

[45] J. Li, G. Schreckenbach, and T. Ziegler, J. Am. Chem. Soc. **117**, 486 (1995).

[46] S. Myllyoja, M. Suvanto, M. Kurhinen, P. Hirva, and T. A. Pakkanen, Surf. Sci. **441**, 454 (1999).

[47] W. H. Baur, Acta Crystallogr., Sect. B **34**, 1751 (1978).

[48] B. A. Morrow and I. A. Cody, J. Phys. Chem. **80**, 1995 (1976).

[49] A. Zecchina and C. O. Aréan, Catal. Rev. **35**, 261 (1993).

[50] B. Domenichini, J. Prunier, M. Petukov, Z. Li, P. J. Møller, and S. Bourgeois, J. Electron Spectrosc. Relat. Phenom. **163**, 19 (2008).

[51] K. E. Lewis, D. M. Golden, and G. P. Smith, J. Am. Chem. Soc. **106**, 3905 (1984).

[52] R. Sniatynsky and D. L. Cedeño, J. Mol. Struct.: THEOCHEM **711**, 123 (2004).

[53] J. C. Kim, G. H. Ha, and B. K. Kim, J. Metastable Nanocryst. Mater. **20-21**, 237 (2003).

[54] M. Huth (private communication).